Proc. Natl. Acad. Sci. USA
Vol. 96, pp. 517–522, January 1999
Cell Biology

Moe1, a conserved protein in *Schizosaccharomyces pombe*, interacts with a Ras effector, Scd1, to affect proper spindle formation

(oncogene/signal transduction/G proteins/microtubules/cell cycle)

CHANG-RUNG CHEN, YING-CHUN LI, JING CHEN, MING-CHIN HOU, PIYI PAPADAKI, AND ERIC C. CHANG*

Department of Biology, New York University, 1009 Main Building, 100 Washington Square East, New York, NY 10003-6688

Edited by Michael H. Wigler, Cold Spring Harbor Laboratory, Cold Spring Harbor, NY, and approved November 24, 1998 (received for review August 25, 1998)

ABSTRACT **In fission yeast, Scd1/Ral1 is a putative guanine nucleotide exchange factor for Cdc42sp and also acts as a Ras1 effector necessary for the regulation of cytoskeleton organization. In this study, we have characterized a protein, Moe1, that binds directly to Scd1. A *moe1* null (Δ) mutant exhibits numerous phenotypes indicative of abnormal microtubule functioning, including an abnormality in the spindle. *moe1*Δ mutants are resistant to microtubule destabilizing agents; moreover, *moe1*Δ rescued the growth defects of tubulin mutants containing unstable microtubules. These results suggest that Moe1 induces instability in microtubules. Biochemical and subcellular localization studies suggest that Moe1 and Scd1 colocalize in the nucleus. Furthermore, loss of function in Scd1 or Ras1 also induced abnormality in the spindle and is synthetically lethal with *moe1*Δ producing cells that lack a detectable spindle. These data demonstrate that Moe1 is a component of the Ras1 pathway necessary for proper spindle formation in the nucleus. Human and nematode Moe1 both can substitute for yeast Moe1, indicating that the function of Moe1 in spindle formation has been conserved substantially during evolution.**

The *ras* protooncogenes encode GTP/GDP binding proteins that are essential elements in signal transduction pathways necessary for the regulation of cell growth and organization of the cytoskeleton (1). Ras proteins can cycle between the GDP and GTP-bound forms, but only the GTP-bound Ras is active. To activate Ras, extracellular signals act through guanine nucleotide exchange factors, which catalyze the exchange of the bound GDP for GTP. Activated Ras in mammalian cells has been shown to interact with the Raf-mitogen-activated protein kinase cascade to regulate cell proliferation (2, 3). The molecular pathways leading to the remodeling of the cytoskeleton, however, have not been firmly established, although they seem to involve the Rho-like GTPases (4).

The fission yeast *Schizosaccharomyces pombe* has one known Ras homolog, Ras1, which participates in at least two distinct signaling events. Ras1 can interact with the Byr2 protein kinase, a member of a mitogen-activated protein kinase cascade, to mediate mating pheromone signaling that is necessary for mating and sporulation (5, 6). In addition, we have identified a second Ras1 effector, Scd1 (shape and conjugation deficiency, also called Ral1; ref. 7), which is a putative guanine nucleotide exchange factor for Cdc42sp, a Rho-like GTPase (6). Our data suggest that Scd1 is necessary for maintaining an elongated cell shape but not for pheromone signaling. In the same study, we isolated Scd2/Ral3 (6, 7), which interacts directly with Scd1. Our data support a model in which Ras1 and Scd2 act cooperatively to regulate the interaction between Scd1 and Cdc42sp. We will refer to the protein complex of Ras1, Scd1, Scd2, and Cdc42sp as SCD. A putative effector for Cdc42sp has been identified, Shk1/Pak1/Orb2, which is a homolog of the mammalian Pak and budding yeast STE20 protein kinase (8–10).

It has been shown that in *ras1*Δ cells, both the actin and microtubule (MT) cytoskeleton appear disorganized (11, 12). However, neither the physiological significance of these observations nor the mechanisms by which Ras1 affects the organization of the cytoskeleton have been fully analyzed. In a separate study (Y-c.L., C-r.C., and E.C.C., unpublished work), we present evidence demonstrating that the Ras1/Scd1 pathway can affect the functioning of the spindle. To further understand the mechanism by which Scd1 affects spindle functioning, here we describe the study of a conserved protein, Moe1. Our data indicate that one of the principal functions of Moe1 is to reduce stability of MTs and that Moe1 and Scd1 can interact in the nucleus to affect spindle formation. Furthermore, we demonstrate that the function of Moe1 in spindle formation has been conserved substantially during evolution as human and nematode Moe1 both can fully substitute for yeast Moe1.

MATERIALS AND METHODS

Parental Strains and Microbial Manipulation. The generic wild-type strain in our laboratory is SP870 (*h*^{90}*, ade6.210, leu1.32, ura4-D18*). Mutant strains containing the *nda2-KM52* and *nda3-KM311* mutations (13) and their parental wild-type strain (*h*$^{-}$*, leu1.32*) were from Paul Nurse (Imperial Cancer Research Fund, London). For clarification we named the wild-type strain from the Nurse lab PN1. The rich and minimal medium were yeast extract medium supplemented with adenine and uracile (YEAU) and minimal medium (14). Hydroxyurea (HU; 11 mM) treatment was essentially as described (15) except that our strains were incubated in HU for 6 hr. Cell viability was determined by plating on YEAU at 30°C.

Yeast Two-Hybrid Screening. The protocols for the screening and the β-galactosidase assay are as described (6). A *Bam*HI fragment of *scd1ΔB* (encoding residues 1–815; ref. 6) was cloned into pVJL11 to create pLBD-SCD1ΔB. Approximately one million cDNA clones were screened. A total of six SCD1ΔB-specific clones were identified, one of which encodes

The publication costs of this article were defrayed in part by page charge payment. This article must therefore be hereby marked "*advertisement*" in accordance with 18 U.S.C. §1734 solely to indicate this fact.

PNAS is available online at www.pnas.org.

This paper was submitted directly (Track II) to the *Proceedings* office.
Abbreviations: MT, microtubule; GFP, green fluorescence protein; SCD, shape and conjugation deficiency; GST, glutathione *S*-transferase; HT, polyhistidine tagged; MTOC, microtubule organization center, TBZ, thiabendazole.
Database deposition**:** The sequence reported in this paper has been deposited in the GenBank database (accession no. AF038568).
*To whom reprint requests should be addressed. e-mail: eric.chang@nyu.edu.

Moe1ΔN. The interaction between the LBD-Scd1ΔB and GAD-Moe1ΔN detected by the β-galactosidase assay was performed for approximately 6 hr at 30°C.

Cloning of *moe1* and Plasmid Constructions. A 4.1-kb *Bam*HI/*Apa*I fragment containing *moe1* was obtained from cosmid no. 637 (16) and cloned into Bluescript to create pBSMOE1. A 1.8-kb *XcmI* and *Bgl*II fragment in pBSMOE1 was swapped with *ura4* to create pMOE1U; similarly, pMOE1L was constructed by replacing *ura4* with *LEU2*. The *Kpn*I site in the polycloning site of pBSMOE1 was converted to a *Pst*I site by a linker. A 4.1-kb *Sac*I/*Pst*I fragment was excised from the resulting plasmid and cloned into pAL (5) to generate pALMOE1. A *Bgl*II fragment of *moe1* was created by PCR and cloned into pARTCM (6) and pTrcHisB (Invitrogen) to create pARCMOE1 and pHTMOE1, which express c-MYC-Moe1 in yeast and HT-Moe1 in bacteria, respectively. To express glutathione *S*-transferase (GST)-Scd1 in *Sf9* cells, a *Bam*HI/*Nhe*I fragment of *scd1* was obtained from pGAD-SCD1 (6) and cloned into a modified pAcG1 (PharMingen) in which the *Sma*I site had been changed to *Nhe*I. pALLT17N was created by swapping the *ura4* in pALUT17N (6) with *LEU2*. The *Bgl*II-moe1 was cloned into pALG (Y-c.L., C-r.C., and E.C.C., unpublished work), which expresses green fluorescence protein (GFP)-Moe1 (GFP:GFP[S65T]; ref. 17) under the control of the *adh1* promoter. pNMTSCD1 (Y-c.L., C-r.C., and E.C.C., unpublished work) allows expression of GFP-Scd1 under the control of a weak *nmt1* promoter (pREP41; ref. 18). The cDNA for CeMoe1 was amplified from the *Caenorhabditis elegans* cDNAs (provided by Michael Hengartner, Cold Spring Harbor Lab, Cold Spring Harbor, NY) to create unique *Pst*I and *Kpn*I sites and cloned into pART1 (19) to generate pCEMOE1. Human *moe1* was amplified from the cDNAs of HeLa cells (from Greg Hannon, Cold Spring Harbor Lab, Cold Spring Harbor, NY) to contain unique *Bam*HI sites and cloned into pARTCM to create pHSMOE1.

Strain Constructions. To delete *moe1*, strain SP870 was transformed with an *Apa*I/*Sac*I fragment released from pMOE1U. Uracile-prototrophic transformants were selected, and the deletion of *moe1* was confirmed by PCR. One of these was named MOE1U and chosen for detailed studies. A *moe1*Δ strain, PNMOE1L, also was created in strain PN1 by using pMOE1L. Diploid cells homozygous for the deletion of *scd1*, *scd2,* and *ras1* were constructed by protoplast fusion of haploid null cells, SPSCD1U, SPSCD2L, and SPRU, respectively (6). The *ras1*Δ *moe1*Δ, *scd2*Δ *moe1*Δ, and *scd1*Δ *moe1*Δ strains used in this study are named R1UME1L, SD2LME1U, and SD1UME1L.

MT Assembly and Stability in Cells. Cells were pregrown at 30°C to early log phase and then transferred to 20°C to grow for an additional 12 hr. For cold shock, cells were transferred to an ice bath, and time points were taken for fixing and immunofluorescence microscopy as described below. To monitor MT polymerization, samples were subjected to cold shock as above for 30 min and then transferred to 20°C.

Immunoprecipitation and Far-Western Analysis. pARC-MOE1 and pALUSCD1 (6) were used to express the c-MYC-tagged Moe1 and the HA1-tagged Scd1, respectively, in a *scd1* mutant, SP870M3 (6). Freshly transformed cells were used for the preparation of lysates. The lysis buffer was 100 mM Pipes, 1 mM $MgSO_4$, 1 mM EGTA, pH 6.9 (20) plus 1% Triton X-100. mAbs 12CA5 and 9E10 and the control mouse IgG were covalently coupled to protein-A beads (6). For the Far-Western analysis, purified proteins were separated by SDS/PAGE and transferred to a nitrocellulose membrane without using methanol in the transfer buffer. The membrane was incubated first in 3% nonfat dry milk in tris-buffered saline (TBS) for 1 hr; after washing, it was incubated with purified His-tagged HT-Moe1 (1 μg/ml in TBS; 0.05% Tween-20; 3% BSA) overnight at 4°C. An anti-T7 antibody from Novagen was used (1:10,000) to detect the presence of HT-Moe1.

Subcellular Localization. The general procedures for immunostaining were as described (14). To visualize MTs, TAT1 (1:5, overnight) was used (21). F-actin was visualized by Rhodamine-phalloidin (Molecular Probes; 20 units/ml, 1 hr). To examine GFP-Moe1 and GFP-Scd1, cells were transformed with pALGMOE1 or pNMTSCD1 and seeded on plates containing 20 μM thiamine. Overexpression of Scd1 induced lethality in *moe1*Δ cells. To achieve the optimal level of expression of GFP-Scd1, cells were inoculated from the thiamine-rich to the thiamine-free medium and allowed to grow at 30°C for 2 days before being fixed (3% formaldehyde, 5 min). Under these conditions, the expression level of GFP-Scd1 was quite low and was detectable in only 30% of the cells. In addition to the nucleus, GFP-Scd1 also appeared at the spindle and cell equator. In a separate study (Y-c.L., C-r.C., and E.C.C., unpublished work), we have examined the localization of GFP-Scd1 in *scd1*Δ cells in which GFP-Scd1 can be expressed to a higher level. In that case, in addition to the described patterns of localization, GFP-Scd1 also could be detected at the cell tips. Therefore, we speculate that to detect GFP-Scd1 in the cell ends, GFP-Scd1 needs to be expressed at a high level.

RESULTS

Isolation and Sequence Analysis of *moe1*. To identify genes encoding proteins that form complexes with Scd1, we carried out a yeast two-hybrid screen using as bait a truncated, but functional, Scd1 (Scd1ΔB; ref. 6). One of the isolated cDNA clones encodes the C-terminal 271 aa of a protein that we named Moe1 for "microtubules overextended," based on the phenotype of the null strains as described below. The protein encoded by the truncated cDNA (Moe1ΔN) interacts specifically with Scd1ΔB but not with Scd2, Ras1, or Cdc42sp. The full-length *moe1* gene was isolated from a cosmid library (16) and contains an uninterrupted ORF capable of encoding a protein of 568 aa. The truncated cDNA, *moe1ΔN,* encodes residues 298–568.

Databank searches revealed two Moe1 homologs in GenBank, one from humans and one from *C. elegans*. The amino acid sequences of these two Moe1 homologs share more than 50% identity with yeast Moe1 throughout the entire coding region. (A sequence alignment created with CLUSTAL is published as supplemental data to this article on the PNAS web site, www.pnas.org.) The *C. elegans* Moe1 homolog contains 574 residues (Cosmid clone R08D7_3; ref. 22); however, the function of this gene has not been characterized. The human Moe1 homolog, eIF3-p66, contains 548 aa and was identified as a protein copurified with the translation initiation protein complex (23). Whether eIF3-p66 actually is involved in translation remains unknown. Surprisingly, no Moe1 homolog is present in *Saccharomyces cerevisiae* although it contains homologs of Ras1, Scd2, Scd1, Cdc42sp (6), and Shk1 (8, 9).

Loss of Function in *moe1* Induces Abnormalities in MTs and Spindle. To study the function of Moe1, *moe1*Δ strains were created in which the entire *moe1* ORF was removed. The resulting cells are viable, but grow less efficiently than wild-type cells as the growth temperature decreases (Fig. 1*A*). At 30°C, the optimal growth temperature for fission yeast, the generation times of wild-type and *moe1*Δ cells were 2.6 ± 0.3 and 3.4 ± 0.2 hr (mean ± SEM, $n = 3$ experiments), respectively. At 20°C, the growth rate of *moe1*Δ cells reduced to about half of wild type (generation time: 11.7 ± 0.2 vs. 6.7 ± 0.5 hr). The morphology of *moe1*Δ cells is also abnormal. Unlike wild-type cells, which are straight and elongated, *moe1*Δ cells are frequently bent and longer and wider (Fig. 1*B*). Unlike *scd1*Δ cells, which are sterile, *moe1*Δ cells are fertile.

Because the cold-dependent growth defects and the presence of bent cells in *moe1*Δ strains resemble phenotypes of mutants defective in MTs (13, 24–26), we performed immu-

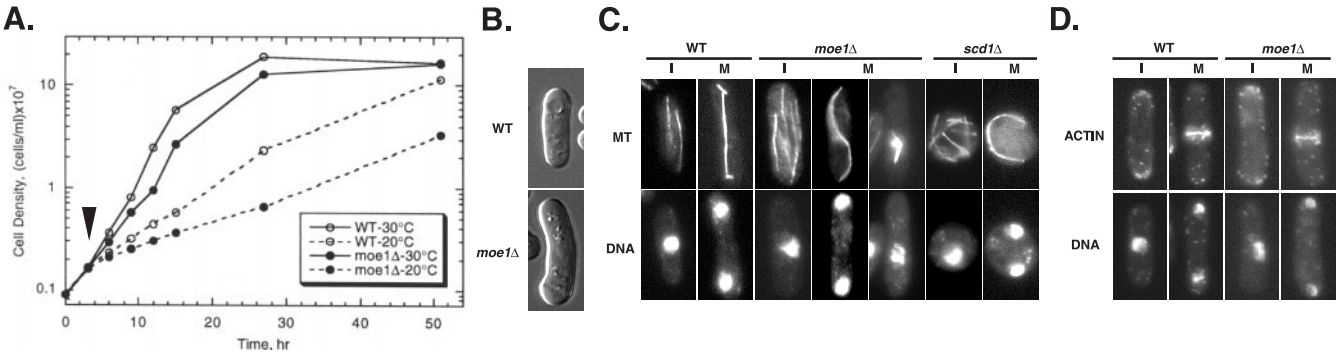

FIG. 1. Growth curve, cell morphology, and MTs of various strains. (*A*) Cells were grown to ≈4 × 10^6 cells/ml at 30°C and then diluted to 1 × 10^6 cells/ml at $t = 0$. After 3 hr (marked by an arrow), cells either were transferred to 20°C or remained at 30°C, and the cell density was monitored over time. (*B*) Cells were pregrown in solid rich medium at 30°C for 24 hr before being examined. The frequency of bent cells was 20%. (*C* and *D*) Cells were grown at 20°C to mid-log phase and subjected to fluorescence microscopy to visualize MTs, F-actin, and DNA. *scd1*Δ and *ras1*Δ cells showed the same abnormal phenotype in MTs at 30°C. I, interphase; M, mitosis. Strains used: SP870 (wild type, WT), MOE1U (*moe1*Δ), SPSCD1U (*scd1*Δ), and SPRN (*ras1*Δ).

nostaining to examine whether MTs are abnormal in *moe1*Δ cells. As shown in Fig. 1*C*, wild-type cells exhibit a typical pattern of interphase MTs with two or three dominant MT bundles extending between the two ends of the cell (27). In *moe1*Δ cells, however, each cell has more MT bundles (Fig. 1*C*). The number of MT bundles per cell was estimated by counting each in various focal planes. *moe1*Δ cells have on average at least 4–6 MT bundles per cell, compared with 2–3 in wild type. *moe1*Δ cells also show abnormalities in the spindle. The two dividing nuclei of a wild-type cell are separated by a single straight spindle (Fig. 1*C*). In *moe1*Δ cells, the spindle in 25% of cells in anaphase appears to be abnormally long and curves within the cell in a distinct "S"-shape (Fig. 1*C*). At a lower frequency (1% of the entire population), we observed what appears to be a fraying V-shaped spindle, which suggests that the MTs in the spindle are not properly interdigitated (Fig. 1*C*; ref. 28). At 30°C, by contrast, these abnormalities in MTs/spindle were rarely detectable.

We also examined the organization of F-actin in *moe1*Δ cells and found no abnormality at either 30°C or 20°C. That is, F-actin is concentrated at the growing ends and the cell equator as observed in wild-type cells (Fig. 1*D*; ref. 27). Hence, we conclude that *moe1*Δ cells have cold-dependent abnormalities in MTs and the spindle, whereas the organization of F-actin does not seem to be visibly altered.

Loss and Gain of Function of Moe1 Affect MT Stability and/or Assembly. We attempted to decipher the influence of Moe1 on the functionality of MTs. As described above, both the number of MT bundles and the length of the spindle increase at 20°C as a result of *moe1*Δ. By using Western blot analysis, we determined that the levels of α tubulins in *moe1*Δ cells was the same as in wild type; thus, it is unlikely that the observed anomaly in MTs and spindle is caused by an overproduction of the α tubulins. Therefore, as an alternative hypothesis, we postulated that Moe1 negatively affects the assembly and/or stability of MTs.

To analyze the stability of MTs in *moe1*Δ cells, we exposed cells to treatments known to promote depolymerization of MT, including cold shock in ice (29) and thiabendazole (TBZ). To quantitate depolymerization of MTs under cold shock, we measured the percentage of cells that have long MTs during the time of the cold shock (Fig. 2*A*). We reasoned that the more stable the MTs are in a cell, the higher the percentage of cells that have long MT bundles and spindle at any given time after the cold shock. Our data show a marked decline in the percentage of cells containing long MT bundles and spindle in wild-type versus *moe1*Δ cells (Fig. 2*A*). In addition, when the cold-shocked cells were allowed to recover at 20°C, we found that MTs also regenerated more readily in *moe1*Δ cells than in wild type (Fig. 2*B*). These data support our model

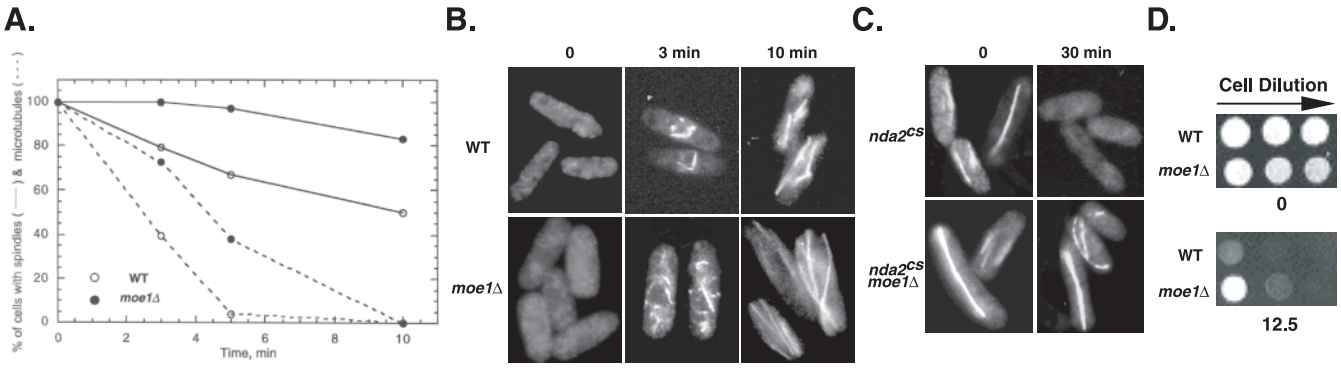

FIG. 2. The effects of loss of function of Moe1 on MT assembly and stability. (*A*) The percentages of cells with either a long MT (one that spans at least half the cell length) or an intact spindle (one that connects the two nuclei) are plotted against time after the cold shock. (*B*) Cells first were cold-shocked in ice for 30 min. The MTs then were examined at various time points after recovery at 20°C. (*C*) α1 tubulin mutant (*nda2*^{cs}) and the α1-tubulin Moe1Δ double mutant cells (*nda2*^{cs} *moe1*Δ) pregrown at 30°C to log phase were shifted to 20°C; the MTs were visualized after 30 min. (*D*) Serial dilutions of cells (1:5) were spotted on yeast extract medium supplemented with adenine and uracile (YEAU) plates (*Materials and Methods*) containing either no or 12.5 μg/ml of thiabendazole. The plates were incubated at 30°C for 3 days. Note that the plating efficiency of *moe1*Δ cells at 30/25°C is only 50% of wild type. We therefore routinely use twice as many *moe1*Δ as wild-type cells for this type of analysis. The wild-type and moe1Δ strains in *A* and *D* were SP870 and MOE1U, respectively, and in *B* were PN1 and PNMOE1L, respectively.

that *moe1*Δ renders MTs more stable and allows them to assemble more readily.

Consistent with the hypothesis that *moe1*Δ leads to a global stabilization of MTs, we found that *moe1*Δ rescued the growth defects of the cold-sensitive α1 (*nda2-KM52*) and β (*nda3-KM311*) tubulin mutants (13) at 20°C. The MTs/spindles in the *moe1*Δ *nda2-KM52* double mutant also appeared more stable than those in the *nda2-KM52* mutant cells at 20°C (Fig. 2*C*). Furthermore, we show that deletion of *moe1* rendered cells more resistant to TBZ (Fig. 2*D*), whereas overexpression of *moe1* rendered cells weakly more sensitive to TBZ (data not shown). Based on these data, we propose that Moe1 negatively affects the assembly and/or stability of MTs.

Moe1 and Scd1 Interact Directly *in Vitro*. The two-hybrid data suggest that Moe1ΔN can form a protein complex with Scd1. We therefore proceeded to investigate whether full-length Moe1 and Scd1 can interact directly by using biochemical methods. Far-Western analysis revealed that poly-histidine tagged Moe1 (HT-Moe1) can interact specifically with immobilized GST-Scd1, but not with the control GST (Fig. 3*A*), demonstrating that Scd1 and Moe1 interact directly *in vitro*. Furthermore, immunoprecipitation experiments revealed that c-Myc epitope-tagged Moe1 coprecipitated with HA1-tagged Scd1 from fission yeast lysates, and vice versa (data not shown). These data indicate that Scd1 directly interacts with Moe1 *in vitro* and suggest a direct interaction between them *in vivo*.

Scd1 Is Required for Proper Nuclear Localization of Moe1. Because Moe1 and Scd1 interact directly *in vitro*, we investigated whether Moe1 and Scd1 colocalize in the cell by using GFP fusion proteins. GFP-Moe1 or GFP-Scd1 both were able to fully complement the phenotypes of *moe1*Δ or *scd1*Δ cells, respectively. As shown in Fig. 3*B*, whereas the GFP control protein was dispersed over the entire cell, GFP-Moe1 appeared predominantly associated with the nucleus throughout the cell cycle. In *S. pombe*, the nuclear envelope does not break down during mitosis so the dividing nuclei remain connected by the nuclear membrane. Moe1 was not present between the two dividing nuclei (data not shown), which suggests that Moe1 is most likely in the nucleus, and not in the nuclear membrane. A functional GFP-Scd1 also can be detected in the nucleus throughout the cell cycle (Y-c.L., C-r.C., and E.C.C., unpublished work) (Fig. 3*B*). More important, the nuclear localization of GFP-Moe1 was dramatically reduced in *scd1*Δ cells (Fig. 3*B*). Together with the biochemical data, we hypothesize that Moe1 and Scd1 colocalize in the nucleus and that Scd1 is essential for proper nuclear localization of Moe1.

Deletion of Both *moe1* and *scd1* Blocks Spindle Formation. We next constructed *moe1*Δ scd1Δ double mutants to define the physiological significance of the physical interaction between Scd1 and Moe1. The *moe1* gene was deleted and replaced with a selectable marker, *LEU2,* in a diploid homozygous for an *scd1* deletion. A total of 52 tetrads from the resulting diploid cells were examined; all produced only two viable spores of four. None of the viable spores were prototrophic for leucine, which suggests that *moe1* and *scd1* double deletions induce synthetic lethality.

To investigate the cause for the synthetic lethality, the diploid cells that are homozygous for *scd1*Δ (*scd1*::*ura4*) and heterozygous for *moe1*Δ (*moe1*::*LEU2*) were induced to sporulate, and the spores were allowed to germinate in minimal medium that would support the "growth" of *scd1*Δ *moe1*Δ cells, but not *scd1*Δ cells. We found that *scd1*Δ *moe1*Δ cells were able to germinate but unable to divide after 24 hr. The majority of these cells (75%) appeared to be in early mitosis with condensed chromosomes but without a spindle (Fig. 4*A*, *Right*). As described above, the spindle in *moe1*Δ cells appears abnormal. In a separate study (Y-c.L., C-r.C., and E.C.C., unpublished work), we found that the spindle in SCD-deficient cells is also abnormal (see also Fig. 1*C*). Therefore, we speculate that the lethality in *scd1*Δ *moe1*Δ cells is the result of the lack of a spindle.

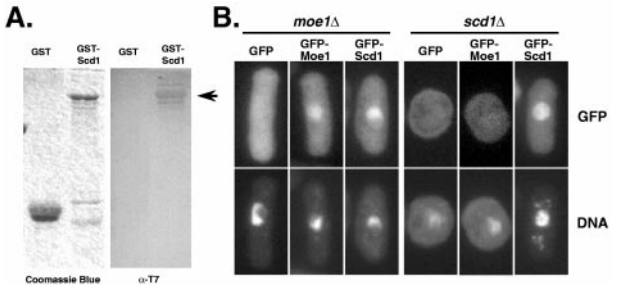

FIG. 3. Physical interaction between Scd1 and Moe1 *in vitro* and *in vivo*. (*A*) Purified GST (3 μg) and GST-Scd1 (1 μg) were separated by SDS/PAGE and transferred to a nitrocellulose membrane. The blot (*Right*) was incubated with purified HT-Moe1 and then analyzed by using an anti-T7 antibody that detected the presence of HT-Moe1 that binds GST-Scd1. The same samples also were stained with Coomassie blue for comparison (*Left*). The protein band corresponding to the GST-Scd1 HT-Moe1 complex is marked by an arrowhead. (*B*) The localization of GFP-Moe1 and GFP-Scd1 in *scd1*Δ (SPSCD1U) and *moe1*Δ (MOE1U) cells was examined after short fixation. Cell samples were counterstained with 4′,6-diamidino-2-phenylindole to view DNA. GFP-Moe1 appeared in the nucleus in >85% of *moe1*Δ cells; in *scd1*Δ cells, however, GFP-Moe1 appeared rather diffused and only <25% of *scd1*Δ cells contained GFP-Moe1 in the nucleus. In contrast, in every *moe1*Δ cell that displayed detectable levels of GFP-Scd1 GFP-Scd1 was always in the nucleus.

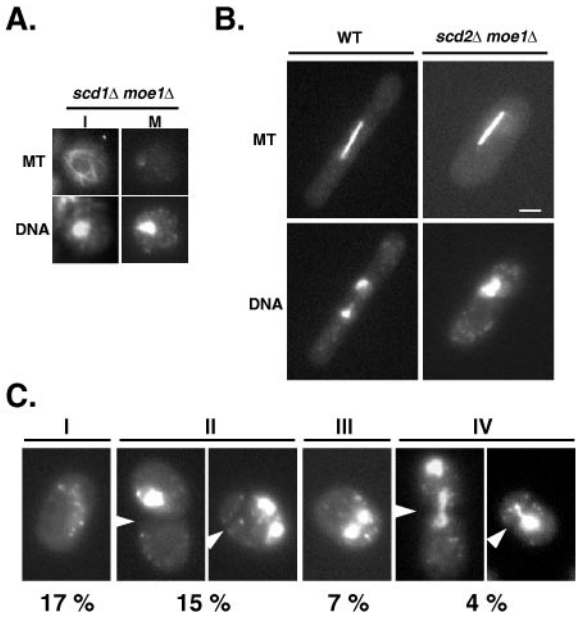

FIG. 4. Loss of function in both Moe1 and SCD affects proper spindle formation. (*A*) Spores of diploid (*scd1*::*ura4*/*scd1*::*ura4* +/*moe1*::*LEU2*) were allowed to germinate in minimal medium that lacks leucine and uracile at 30°C. Cells were immunostained after 24 hr. The majority of cells (>75%) appear to accumulate in early M phase (*Right*), and the rest were still in interphase (*Left* for comparison). (*B*) Separation of chromosomes in cells that contain a spindle of 6 μm. (Scale bar = 3 μm.) (*C*) Aberrant morphology of synchronized *scd2*Δ *moe1*Δ cells (*I–IV*) after two generations at 20°C. Cells were fixed in methanol and stained with 4′,6-diamidino-2-phenylindole. (*I*) Cells with no or only traces of DNA signal. (*II*) Cells with unequal number of nuclei in the two cell compartments separated by a septum. (*III*) Binucleate cells without a spindle (MT staining is not shown). (*IV*) Cells with at least one of the nuclei "cut" by the septum. The position of the septum is indicated by an arrowhead. The frequency at which the abnormal cells occurred is indicated. The strains used in this study were: SP870 (wild type, WT), SD1UME1L (*scd1*Δ *moe1*Δ), and SD2LME1U (*scd2*Δ *moe1*Δ).

Deletion of *moe1* in Other SCD Loss-of-Function Mutants Also Blocks Proper Spindle Formation. Scd1 is part of a protein complex that contains at least three other proteins, Ras1, Scd2, and Cdc42sp. Hence, one would expect that components interacting with Scd1 also would interact with Ras1, Scd2, or Cdc42. In support of this hypothesis, we found that deletion of *ras1* induced synthetic lethality in *moe1*Δ cells, and the terminal phenotype of these cells is indistinguishable from that of *scd1*Δ *moe1*Δ cells (data not shown).

Deletion of *scd2* also created a synthetic lethality in *moe1*Δ cells, but, unlike *scd1*Δ *moe1*Δ cells, which are not viable at 30°C, *scd2*Δ *moe1*Δ cells grow but very slowly. At 20°C, however, the *scd2*Δ *moe1*Δ strain cannot form colonies. To investigate whether these *scd2*Δ *moe1*Δ cells are also defective in spindle formation, we first examined the percentage of synchronized cells that have a detectable spindle.

Cells were synchronized at 30°C by hydroxyurea, and then released from the blockage and allowed to grow at 20°C. We counted over time the percentage of cells at 20°C that had entered anaphase (the anaphase index), as judged by the presence of two dividing nuclei lying along the cell body by using 4′,6-diamidino-2-phenylindole staining. As the anaphase index peaked, approximately 56% of wild-type and *scd2*Δ cells and 47% of *moe1*Δ cells had a spindle; by contrast, in *scd2*Δ *moe1*Δ cells, only 24% had a spindle. Because the chromosomes in the majority of *scd2*Δ *moe1*Δ cells (60%) were condensed, the lack of a detectable spindle is unlikely to result from a mitotic block caused by the lack of chromosome condensation. These data support the hypothesis that the ability to generate a spindle is substantially inhibited in *scd2*Δ *moe1*Δ cells. Furthermore, for those *scd2*Δ *moe1*Δ cells that did make a long spindle of 6 μm, more than 80% could not efficiently separate the chromosomes so there was only a single DNA mass (Fig. 4*B*). In contrast, in the majority of wild-type, *scd2*Δ, or *moe1*Δ cells (>80%), the two sister-chromatids can fully separate (Fig. 4*B*). These data suggest that if a spindle is generated in *scd2*Δ *moe1*Δ cells, it cannot separate chromosomes efficiently. Thus, we conclude that *scd2*Δ *moe1*Δ cells are defective in the generation of a functional spindle.

To examine the terminal phenotype of *scd2*Δ *moe1*Δ cells, the cultures were kept at 20°C for one more generation. We observed no appreciable loss of viability in wild-type, *scd2*Δ, and *moe1*Δ cells after two generations (>80% viable). In contrast, more than 70% of *scd2*Δ *moe1*Δ cells were inviable with deformities that can be grouped into four major categories (Fig. 4*C*). We observed deformities indistinguishable from those shown in Fig. 4*C* in an asynchronous culture of *scd2*Δ *moe1*Δ cells at 20°C, indicating that these abnormalities are not artifacts caused by hydroxyurea. The accumulation of these abnormal cells occurs frequently in mutant strains defective in chromosome disjunction (26). One explanation is that septation/cytokinesis in *S. pombe* still can take place even though the chromosomes are not properly segregated, which ultimately results in uneven distribution of chromosomes in the two daughter cells. We conclude that the lethality in *scd2*Δ *moe1*Δ cells is caused by the absence of a functional spindle, which results in chromosome loss.

Deletion of *cdc42sp* alone induces lethality (30). To test whether a defective Cdc42sp can impart lethality to *moe1*Δ cells, we overexpressed a dominant negative Cdc42sp (Cdc42sp[T17N]; refs. 6, 8, and 9), and found that it, too, induced lethality in *moe1*Δ cells, producing abnormal cells indistinguishable from those in Fig. 4*C*.

On the basis of these double mutant studies, we conclude that SCD and Moe1 both are required for the construction of a functional spindle. In combination with *moe1*Δ, deletion of *scd1* or *ras1* appears to lead to a complete loss of a detectable spindle, whereas deletion of *scd2* or overexpression of Cdc42sp[T17N] severely inhibits spindle formation and proper chromosome segregation.

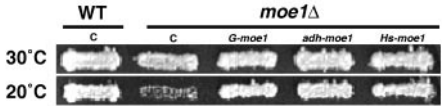

FIG. 5. Moe1 function is conserved in evolution. Shown here are cell patches generated by replica plating containing various plasmids growing at 30°C for 2 days or at 20°C for 4 days. The plasmids tested were: pARTCM (C, empty vector), pALMOE1 (*G-moe1*, expression controlled by the genomic *moe1* promoter), pARCMOE1 (*adh-moe1*, expression controlled by the *adh1*-promoter), and pHSMOE1 (*Hs-moe1*, expression of human *moe1* controlled by the *adh1*-promoter). Strains used were SP870 (wild type, WT) and MOE1U.

Moe1 Function Is Conserved in Evolution. To test whether the function of Moe1 is conserved in evolution, we investigated the effects of overexpressing human Moe1 on the phenotypes of *S. pombe moe1*Δ cells. Human Moe1 was able to rescue all the described phenotypes of *moe1*Δ cells: namely, the abnormal cell morphology, the presence of V- and S-shaped spindle, and the cold-dependent growth defect (Fig. 5). These results suggest that human Moe1 can affect the functioning of MTs in a manner very similar to that of yeast Moe1. Furthermore, human Moe1 also rescued the lethality of *scd2*Δ *moe1*Δ cells (data not shown), suggesting that human Moe1 also can interact with the Ras1/Scd1 pathway. The *C. elegans* Moe1 also rescued the phenotypes of *moe1*Δ cells (data not shown). These data demonstrate that the function of Moe1 is highly conserved in evolution. We suggest that the *C. elegans* and human Moe1 should be named CeMoe1 and HsMoe1, respectively.

DISCUSSION

In this report, we describe the characterization of a highly conserved gene from fission yeast, *moe1*. Biochemical and subcellular localization studies suggest that Moe1 and a Ras1 effector, Scd1, interact directly in the nucleus. We conclude from the genetic analysis of Moe1 SCD double mutants that Moe1 is a key component of the Ras1/Scd1 signaling pathway necessary for proper spindle formation.

Judging from the phenotypes of *moe1*Δ cells, we conclude that the deletion of *moe1* primarily affects the function of MTs, but not the organization of F-actin. Furthermore, we determined that one of the principal functions of Moe1 is to destabilize MTs. The exact molecular mechanism by which this process occurs, however, is unresolved in this study. Increasing evidence suggests that motor proteins in the family of kinesin and dynein can play a key role in reducing the stability of MTs (31). In budding yeast, for example, a loss of function in a dynein-related motor protein, Dyn1 (32), induces cold-dependent spindle defects, and the *dyn1* mutant cells are resistant to a MT-destabilizing drug, benomyl. These phenotypes are reminiscent of the phenotypes of *moe1*Δ cells. Hence, we speculate that Moe1 can affect MT stability through the action of motor proteins. Cold conceivably can retard the mobility of these motor proteins to reduce their effectiveness, which could explain why the phenotypes of *moe1*Δ cells are manifested predominantly in the cold. We note that our data are insufficient to judge whether the lack of Moe1 function promotes polymerization of MTs directly or it influences the organization and/or integrity of MTs, which then leads to an apparent increase in MT stability.

It is possible that persistent MTs block MT remodeling necessary for the generation of a functional spindle. Consistent with this hypothesis, it has been shown that the spindle of *S. pombe* is composed of several types of MTs, the length and number of which change dynamically during mitosis (33). It is conceivable that such MT morphogenesis would require cycles of MT assembly and disassembly in which Moe1 participates.

Subcellular localization studies illustrate that Moe1 and Scd1 can concentrate in the nucleus. The nucleus of *S. pombe* has been suggested to play an essential role in the regulation of MT functioning throughout the cell cycle. Interphase MTs that are experimentally disassembled regenerate from near the nucleus, suggesting the presence of microtubule organization centers (MTOCs) in or by the nucleus (ref. 29; wild-type cells in Fig. 2*B*). The generation of the spindle requires the spindle pole bodies, the yeast MTOCs responsible specifically for spindle formation, to integrate into the nuclear envelope. The importance of the nucleus in the regulation of MT assembly and stability is further underscored by the finding that essential constituents for the MTOCs, such as γ-tubulin (34), can be found in the nucleus. It is possible that the Moe1–Scd1 complex may exert at least part of its effects on MT assembly/stability by interacting with components of the MTOCs that are associated with the nucleus.

Our data show that the nuclear localization of Moe1 is markedly reduced in *scd1*Δ cells, whereas the nuclear localization of GFP-Scd1 was not markedly altered in *moe1*Δ cells. This result suggests that part of the function of Scd1 is to maintain Moe1 in the nucleus. In this scenario, Scd1 acts in a manner similar to other guanine nucleotide exchange factors, such as Sos (35), to assemble elements into a single protein complex that apparently can maximize the efficiency of signal transduction. However, the function of Scd1 in the regulation of spindle formation is unlikely to be limited to controlling the subcellular localization of Moe1. In a separate study, we show that Scd1 also can associate with the spindle (Y-c.L., C-r.C., and E.C.C., unpublished work). As shown here, however, Moe1 does not seem to associate with the spindle. Furthermore, GFP-Scd1 remains associated with the spindle in *moe1*Δ cells (unpublished results). These observations suggest that Scd1 can interact with the spindle and that the association between Scd1 and the spindle is independent of Moe1. Thus, in addition to recruiting Moe1 to the nucleus, Scd1 may anchor to the spindle to recruit other molecules necessary for spindle formation. Furthermore, because deletion of both *moe1* and *scd1* create a phenotype that is more severe than either single deletion, it is possible that Moe1 or Scd1 interacts with additional molecules to affect spindle formation.

A databank search has identified full-length sequences in *C. elegans* and humans that are more than 50% identical to Moe1. It is enticing to speculate that these Moe1 homologs also interact with the Ras pathway and MTs. In support of this hypothesis, we have shown that both nematode and human Moe1 can substitute for the function of yeast Moe1. Moreover, human Cdc42 (Cdc42Hs) has been shown to affect the functioning of the MTOCs. For example, helper T cells reorient MTOCs toward the antigen-presenting cells, which ultimately leads to a contact between the two cell types. Stowers and coworkers (36) have shown that this process can be blocked by the dominant negative Cdc42Hs. Finally, we note that the elevated levels of MT stability/assembly in *moe1*Δ cells resemble the centrosome hypertrophy observed in tumors in which MTs assemble robustly because of an increase in the number and size of the centrosomes (37). One can envision that centrosome hypertrophy also can lead to improper chromosome segregation, similar to that observed in yeast cells deficient in Moe1 and SCD, which would accelerate malignant transformation.

We thank Richard McCombie for assisting with the cosmid screening, Deirdre Sawinski, I-Ren Chen, Miki Onda, Laurie Wang, Liang-Tung Yang, and members of the Fitch and Small labs for technical assistance, and Leonille Douglas, Philip Benfey, Gloria Coruzzi, and Kathy Mauro for discussion. We truly appreciate indicated colleagues for providing materials critical for our work. This project was supported by Research Challenge Funds and a Whitehead Fellowship from New York University and grants from the American Cancer Society. We are especially grateful to the anonymous reviewers for our grant proposals who supported our project in its early stage (during which Moe1 was named Fim1).

1. Lowy, D. R. & Willumsen, B. M. (1993) *Annu. Rev. Biochem.* **62,** 851–891.
2. Van Aelst, L., Barr, M., Marcus, S., Polverino, A. & Wigler, M. (1993) *Proc. Natl. Acad. Sci. USA* **90,** 6213–6217.
3. Vojtek, A. B., Hollenberg, S. M. & Cooper, J. (1993) *Cell* **74,** 205–214.
4. Van Aelst, L. & D'Souza-Schorey, C. (1997) *Genes Dev.* **11,** 2295–2322.
5. Wang, Y., Xu, H. P., Riggs, M., Rodgers, L. & Wigler, M. (1991) *Mol. Cell. Biol.* **11,** 3554–3563.
6. Chang, E. C., Barr, M., Wang, Y., Jung, V., Xu, H. & Wigler, H. M. (1994) *Cell* **79,** 131–141.
7. Fukui, Y. & Yamamoto, M. (1988) *Mol. Gen. Genet.* **215,** 26–31.
8. Marcus, S., Polverino, A., Chang, E., Robbins, D., Cobb, M. H. & Wigler, M. (1995) *Proc. Natl. Acad. Sci. USA* **92,** 6180–6184.
9. Ottilie, S., Miller, P. J., Johnson, D. I., Creasy, C. L., Sells, M. A., Bagrodia, S., Forsburg, S. L. & Chernoff, J. (1995) *EMBO J.* **14**, 5908–5919.
10. Verde, F., Wiley, D. J. & Nurse, P. (1998) *Proc. Natl. Acad. Sci. USA* **95,** 7526–7531.
11. Pichová, A. & Streiblová, E. (1992) *Exp. Mycol.* **16,** 178–187.
12. Pichová, A., Kohlwein, S. D. & Yamamoto, M. (1995) *Protoplasma,* **188** 252–257.
13. Umesono, K., Toda, T., Hayashi, S. & Yanagida, M. (1983) *J. Mol. Biol.* **168,** 271–284.
14. Alfa, C., Fantes, P., Hyams, J., McLeod, M. & Warbrick, E. (1993) *Experiments with Fission Yeast* (Cold Spring Harbor Lab. Press, Plainview, NY).
15. Moser, M. J., Flory, M. R. & Davis, T. N. (1997) *J. Cell Sci.* **110,** 1805–1812.
16. Mizukami, T., Chang, W. I., Garkavtsev, I., Kaplan, N., Lombardi, D., Matsumoto, T., Niwa, O., Kounosu, A., Yanagida, M., Marr, T. G. & Beach, D. (1993) *Cell* **73,** 121–132.
17. Heim, R., Cubitt, A. B. & Tsien, R. (1995) *Nature (London)* **373,** 663–664.
18. Schmid, B. G. & Maundrell, K. (1993) *Gene* **123,** 131–136.
19. McLeod, M., Stein, M. & Beach, D. (1987) *EMBO J.* **6,** 729–736.
20. Solomon, F., Connell, L., Kirkpatrick, D., Praitis, V. & Weinstein, B. (1992) *Methods for Studying the Yeast Cytoskeleton* (Oxford Univ. Press, Oxford).
21. Woods, A., Sherwin, T., Sasse, R., MacRae, T. H., Baines, A. J. & Gull, K. (1989) *J. Cell Sci.* **93,** 491–500.
22. Sulston, J., Du, Z., Thomas, K., Wilson, R., Hillier, L., Staden, R., Halloran, N., Green, P. Thierry-Mieg, J., Qiu, L., *et al.* (1992) *Nature (London)* **356,** 37–41.
23. Asano, K., Vornlocher, H.-P., Richter-Cook, N. J., Merrick, W. C., Hinnebusch, A. G. & Hershey, J. W. B. (1997) *J. Biol. Chem.* **272,** 27042–27052.
24. Toda, T., Umesono, K., Hirata, A. & Yanagida, M. (1983) *J. Mol. Biol.* **168,** 251–270.
25. Snell, V. & Nurse, P. (1994) *EMBO J.* **13,** 2066–2074.
26. Verde, F., Mata, J. & Nurse, P. (1995) *J. Cell Biol.* **131,** 1529–1538.
27. Alfa, C. E. & Hyams, J. S. (1990) *J. Cell Sci.* **96,** 71–77.
28. Su, S. S. Y. & Yanagida, M. (1997) in *The Molecular and Cellular Biology of the Yeast Saccharomyces: Cell Cycle and Cell Biology,* eds. Pringle, J. R., Broach, J. R. & Jones, E. W. (Cold Spring Harbor Lab. Press, Plainview, NY), pp. 765–825.
29. Mata, J. & Nurse, P. (1997) *Cell* **89,** 939–949.
30. Miller, P. J. & Johnson, D. I. (1994) *Mol. Cell. Biol.* **14,** 1075–1083.
31. Stearns, T. (1997) *J. Cell Biol.* **138,** 957–960.
32. Cottingham, F. R. & Hoyt, M. A. (1997) *J. Cell Biol.* **138,** 1041–1053.
33. Ding, R., McDonald, K. L. & McIntosh, J. R. (1993) *J. Cell Biol.* **120,** 141–151.
34. Ding, R., West, R. R., Morphew, M., Oakley, B. R. & McIntosh, J. R. (1997) *Mol. Biol. Cell* **8,** 1461–1479.
35. Schlessinger, J. (1994) *Trends Biochem. Sci.* **18,** 273–275.
36. Stowers, L., Yelon, D., Berg, L. J. & Chant, J. (1995) *Proc. Natl. Acad. Sci. USA* **92,** 5027–5031.
37. Lingle, W. L., Lutz, W. H., Ingle, J. N., Maihle, N. J. & Salisbury, J. L. (1998) *Proc. Natl. Acad. USA* **95,** 2950–2955.